

Optimized Compilation of Logical Clifford Circuits

Alexander Popov^{*†}, Nico Meyer^{*‡}, Daniel D. Scherer^{*}, and Guido Dietl[†]

^{*}Fraunhofer IIS, Fraunhofer Institute for Integrated Circuits IIS, Nürnberg, Germany

[†]University of Würzburg, Professorship of Satellite Communication and Radar Systems, Würzburg, Germany

[‡]Pattern Recognition Lab, Friedrich-Alexander-Universität Erlangen-Nürnberg, Erlangen, Germany

Abstract—Fault-tolerant quantum computing hinges on efficient logical compilation, in particular, translating high-level circuits into code-compatible implementations. Gate-by-gate compilation often yields deep circuits, requiring significant overhead to ensure fault-tolerance. As an alternative, we investigate the compilation of primitives from quantum simulation as single blocks. We focus our study on the $[[n, n-2, 2]]$ code family, which allows for the exhaustive comparison of potential compilation primitives on small circuit instances. Based upon that, we then introduce a methodology that lifts these primitives into size-invariant, depth-efficient compilation strategies. This recovers known methods for circuits with moderate Hadamard counts and yields improved realizations for sparse and dense placements. Simulations show significant error-rate reductions in the compiled circuits. We envision the approach as a core component of peephole-based compilers. Its flexibility and low hand-crafting burden make it readily extensible to other circuit structures and code families.

Index Terms—Quantum Computing, Quantum Simulation Kernel (QSK), Quantum Error Correction (QEC), Clifford Circuits, Logical Circuit Compilation

I. INTRODUCTION

Quantum error correction (QEC) is essential for scaling quantum computers and remains a primary bottleneck [1], [2]. A key challenge is efficient logical compilation: mapping circuits to a chosen code with low undetected error while respecting architectural constraints and minimizing depth and spacetime volume [3], [4]. For leading approaches such as the surface code, gate-by-gate compilation inflates resource requirements because logical gates require repeated stabilizer measurement rounds and code-deformation primitives (e.g., lattice surgery), introducing routing, ancillas, and synchronization barriers [5], [6]. Global optimization that exploits commutation and shared parity measurements is therefore crucial to remove unnecessary cycles and active patches, reduce logical depth and spacetime volume, and align with surrounding subroutines such as distillation and syndrome extraction.

Building on the stabilizer framework and early fault-tolerant gate realizations [7], [8], and on binary symplectic representations of Clifford operations with encoded Paulis [9], *Rengaswamy et al.* [10] introduced a symplectic-geometry synthesis that enumerates compatible logical realizations for arbitrary stabilizer codes. While this *logical Clifford synthesis* (LCS) approach exposes the full design space, its search space grows

The research was supported by the Bavarian Ministry of Economic Affairs, Regional Development and Energy with funds from the Hightech Agenda Bayern via the project BayQS and in parts by the German Federal Ministry of Research, Technology and Space, funding program Quantum Systems, via the project Q-GeneSys, grant number 13N17389.

Correspondence to: alexander.popov.res@proton.me

combinatorially with circuit width and gate count, making it costly to isolate low-depth, low-volume realizations at scale. More recently, *Chen and Rengaswamy* [11], [12] proposed a complementary, algorithm-tailored *solve-and-stitch* (SAS) formulation to hand-craft depth-efficient logical implementations of Clifford quantum simulation kernels (C-QSKs) [13]—an important primitive in quantum simulation algorithms—on the $[[n, n-2, 2]]$ code family [7]. This reduces compilation complexity via scalable templates but requires substantial manual design and, as we show, can be suboptimal in some regimes.

As in Refs. [10]–[12], [14], we focus on C-QSK, which arise as well-defined subroutines inside larger quantum circuits and can be optimized independently of surrounding non-Clifford gates. Our constructions thus serve as logical peephole optimizations [15], [16]: we identify and replace Clifford sub-circuits with depth-optimized encoded realizations on the chosen code family. Concretely, we mine small instances with LCS [10] to discover low-depth compilation primitives, then lift these patterns into strategies that scale to arbitrary system sizes while respecting code constraints. This narrows the search to structurally meaningful candidates, reduces hand-crafting, and improves upon SAS [11], [12] in edge regimes.

Main Contributions of this Work. We claim and summarize the main contributions of our paper as follows:

- I. We systematically mine the design space of small C-QSK instances using LCS, uncovering depth-favorable compilation primitives and distilling them into closed-form sequencing rules for the $[[n, n-2, 2]]$ family.
- II. We generalize these components into scalable compilation strategies that synthesize circuits of arbitrary size with reduced manual effort, enabling streamlined extensions to other code families and circuit structures.
- III. We introduce proof techniques that verify correctness by checking the required logical Pauli constraints and stabilizer preservation.
- IV. We empirically validate the derived strategies under noise simulation, demonstrating reduced depth and higher success rates; the largest gains over SAS appear in edge regimes of C-QSK.

Overall, we provide a mathematical framework for the efficient development of depth-optimized compilation strategies, tailored for peephole optimization of Clifford sub-circuits.

The remainder of this paper is structured as follows: In Sec. II, we establish preliminaries on stabilizers, Pauli constraints, and the C-QSK. We furthermore position our work in the

context of quantum compilation and summarize necessary insights from prior work, in particular regarding the LCS and SAS approaches. In Sec. III, we use the aforementioned LCS algorithm to identify promising compilation primitives on tractable system sizes. The identified structures are generalized in Sec. IV to arbitrary system sizes, and we furthermore prove correctness. In particular, we re-discover the SAS approach under certain structural assumptions on the C-QSK, while we identify improved strategies for relaxed restrictions. In Sec. V, we perform an empirical evaluation of the discovered compilation strategies and quantify improvements over SAS. Finally, in Sec. VI, we position our results in the greater context of fault-tolerant quantum computing (FTQC), discuss limitations, and identify potential for future extensions.

II. PRELIMINARIES AND PRIOR WORK

We focus on Clifford sub-circuits within larger algorithms. Clifford circuits map the Pauli group \mathcal{P}_n onto itself. As every quantum state decomposes into Pauli operators, a Clifford circuit is fully characterized by its action on the Pauli basis. It suffices to track the generators $X_{1:k}$ and $Z_{1:k}$; the transformations of $Y_{1:k}$ follow from $Y_i = X_i Z_i$ for $i \in \{1, \dots, k\}$. We call these transformation rules the *Pauli constraints*. A logical implementation on any $[[n, k, d]]$ stabilizer code, where n is the number of physical qubits, k the number of encoded logical qubits, and d the code distance, must satisfy two key requirements:

1) *Logical Pauli Constraints*: The circuit must mimic the mapping relations of the Clifford circuit for the k logical Pauli generators \bar{X}_i and \bar{Z}_i . These logical constraints are given by:

$$\begin{aligned} \bar{X}_i &\mapsto C_i^X(\bar{X}_{1:k}, \bar{Y}_{1:k}, \bar{Z}_{1:k}), \\ \bar{Z}_i &\mapsto C_i^Z(\bar{X}_{1:k}, \bar{Y}_{1:k}, \bar{Z}_{1:k}). \end{aligned} \quad (1)$$

Here, $\bar{X}_{1:k}$ abbreviates $\bar{X}_1 \dots \bar{X}_k$, and C_i^X and C_i^Z describe how each Pauli operator transforms under the C-QSK circuit. As the logical \bar{X}_i and \bar{Z}_i operations on the $[[n, n-2, 2]]$ code family are $X_i X_{i+1}$ and $Z_{i+1} Z_n$ [7], [17], respectively, we define the embedding $\mathcal{E} : [k] \rightarrow \{2, \dots, n-1\}$ by $\mathcal{E}(i) = i+1$ to simplify notation.

2) *Stabilizer Preservation*: To enable reliable error correction and detection, the logical Clifford circuit must preserve the stabilizer group \mathcal{S} of the code, meaning it maps \mathcal{S} back onto itself under conjugation. This preservation of the stabilizer group ensures that the syndrome measurements remain valid throughout the computation.

Because globally optimal compilation is impractical, one typically uses local peephole-based optimizations [15], [16]. These local blocks appear in quantum simulation kernels repeating, frequently executed subroutines of quantum simulation algorithms [13]. We focus on Clifford quantum simulation kernels (C-QSKs), where $R_z(\theta)$ is restricted to $P = R_z(\frac{\pi}{2})$, as shown in Fig. 1. For a fixed system size, these circuits differ only in the number and locations of Hadamard gates; let $I_h \subseteq \{1, \dots, k\}$ denote the set of qubit indices with Hadamards, where h is its cardinality.

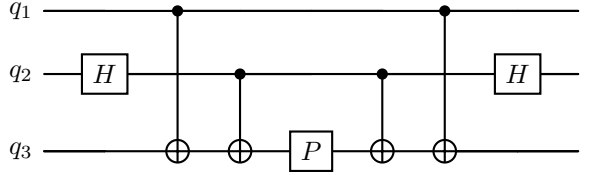


Fig. 1: Clifford quantum simulation kernel (C-QSK) on three qubits with a Hadamard gate only on the second qubit, i.e. $I_h = \{2\}$ and $|I_h| = 1$.

To date, logical compilation is largely gate-by-gate, with few exceptions for specialized circuit classes like IQP circuits [18], [19]. While broader QEC tasks have seen rapid progress—e.g., ML-based encodings [20], [21] and decoders [22]—efficient, code-specific compilation remains underexplored. Among the few targeted methods are LCS and SAS, which we adopt and summarize below.

A. The Logical Clifford Synthesis (LCS) Algorithm

The LCS algorithm introduced in [10] generates all logical realizations of any Clifford circuit on any quantum code. To achieve that, first, the Pauli constraints of the underlying circuit are transformed into binary symplectic equations by means of the so-called m -qubit operator

$$D(a, b) = X^{a_1} Z^{b_1} \otimes \dots \otimes X^{a_m} Z^{b_m}, \quad (2)$$

with $a = [a_1, \dots, a_m]$, $b = [b_1, \dots, b_m] \in \mathbb{F}_2^m$, $m \in \mathbb{N}$. Every Pauli operator can be seen as such an m -qubit operator and therefore can be associated with the two binary vectors a and b . Hence, the Pauli constraints can be interpreted as mappings from one set of binary vectors to another, which gives rise to the system of linear equations

$$[a'_i, b'_i] = [a_i, b_i] F, \quad i \in \{1, \dots, k\}, \quad (3)$$

where k is the system size for the respective Clifford circuit.

The symplectic solution F is then decomposed into a product of so-called elementary forms, which correspond to specific elementary quantum gates. This product therefore defines a Clifford quantum circuit for each symplectic solution obtained with the LCS algorithm. It is important to mention that the decomposition into elementary forms is not unique and, therefore, variations in the realized circuits are possible. By design, the LCS algorithm iterates all possible solutions of the system of equations. While this in principle allows to search for compilations that are optimal w.r.t. a given metric, the solution space grows super-exponentially in the stabilizer rank: for a general $[[n, k, d]]$ stabilizer code, a given logical Clifford circuit admits $2^{r(r+1)/2}$ symplectic solutions with $r = n - k$. To the best of our knowledge, no methods are known to filter for solutions with specific properties already at the solving stage. However, for the $[[n, n-2, 2]]$ code family considered in this work, there are only $2^3 = 8$ solutions, which allows for an exhaustive analysis of the solutions.

$\prod_{i \in \mathcal{E}(\bar{I}_h)} \text{CX}_{i \rightarrow 1} \cdot \left(\prod_{j \in \mathcal{E}(I_h)} \text{CX}_{i \rightarrow j} \right)$	$\prod_{j \in \mathcal{E}(I_h) \cup \{1\}} \text{CX}_{n \rightarrow j}$	$\prod_{i \in \mathcal{E}(I_h) \cup \{1\}} H_i$	$\prod_{i \in \mathcal{E}(I_h) \cup \{1\}} P_i$	$\prod_{i \in \mathcal{E}(I_h)} \text{CZ}_{1,i}$	$\prod_{i \in \mathcal{E}(I_h)} \prod_{j \in \mathcal{E}(I_h) \setminus \{i\}} \text{CZ}_{i,j}$	$\prod_{i \in \mathcal{E}(I_h) \cup \{1\}} H_i$	$\prod_{i \in \mathcal{E}(\bar{I}_h) \cup \{n\}} P_i$	$\prod_{i \in \mathcal{E}(\bar{I}_h)} \left(\prod_{j \in \mathcal{E}(\bar{I}_h) \setminus \{i\}} \text{CZ}_{i,j} \right) \text{CZ}_{i,n}$
--	---	---	---	--	---	---	---	--

Fig. 2: Full sequencing rule obtained by the \mathcal{C}_{mid}^H compilation strategy, which is equivalent to the SAS from [11] (up to re-formulations with different notation). Operations highlighted in gray occur only for odd Hadamard configurations. The embedding function is given by $\mathcal{E} : [k] \rightarrow \{2, \dots, n-1\}$ with $\mathcal{E}(i) = i+1$.

B. The Solve-and-Stitch (SAS) Algorithm

The SAS algorithm described in [11], [12] is a specialized approach in order to obtain a logical realization of the C-QSK on the $[[n, n-2, 2]]$ code family. Intuitively, following the explicit form of the logical operators $\bar{X}_i = X_1 X_{i+1}$, $\bar{Z}_i = Z_{i+1} Z_n$, the Pauli constraints are written in a closed form giving rise to compilation strategies that generalize to arbitrary system sizes k .

The concrete procedure of the SAS algorithm is the following: given the logical-to-physical X - and Z -mappings, one first constructs, for each gate in the C-QSK separately, a circuit that realizes the corresponding mapping relation (the *solve* step). These individual logical realizations are then *stitched* together, typically by removing duplicate gates, so that the resulting circuit simultaneously fulfills all required logical-to-physical mapping relations. The combined circuit is subsequently checked for stabilizer preservation and, if necessary, adjusted. Applying this procedure yields a compilation strategy which we summarize using a slightly modified notation in Fig. 2. This procedure, however, requires substantial manual effort for the construction of the individual mapping circuits, the stitching such that the combined circuit satisfies all constraints simultaneously, and the adjustments to ensure stabilizer preservation.

III. DEPTH-OPTIMIZED COMPILE PRIMITIVES FOR SMALL SYSTEMS

Our objective is to design compilation routines for C-QSK circuits that produce physical realizations with shallow depth, and thus presumably reduced error susceptibility. Towards this goal, we first employ the above-discussed LCS algorithm to systematically analyze the solution space of small circuit instances. As discussed above, for the $[[n, n-2, 2]]$ code family LCS produces eight solutions, i.e. eight candidates for compilation primitives.

Apart from the number of qubits, the C-QSKs which we consider only differ by the number and position of the Hadamard gates. For this purpose, for small system sizes with $2 \leq k \leq 8$ logical qubits, we exhaustively enumerated all possible Hadamard placements. For medium-sized systems $10 \leq k \leq 20$, such an exhaustive sweep would have been computationally infeasible, since the number of placements grows combinatorially in k . In this case, we restrict the analysis to 10 randomly sampled placements per Hadamard-count, which we found to still provide a representative picture of the circuit behavior.

From this analysis, we found that the depth of the logical realization (mainly driven by the two-qubit count, as single-qubit gates are compiled in compact layers) strongly depends on which of the eight solutions from the LCS algorithm is selected. Interestingly, for four of the solutions, the depth is invariant w.r.t. the actual Hadamard positioning and only depends on the count h . The other four solutions show a large spread of depth over different Hadamard placements. As the minimal depth among these realizations is in general significantly higher than for the well-behaved solutions, we focus only on these for our further analysis.

Extending our analysis to a system size of $k = 20$ in Fig. 3, we find that different solutions perform particularly well for different C-QSK structures. One solution produces minimal-depth circuits for moderate Hadamard counts of about 5 to 15, which we refer to as solution \mathcal{S}_{mid}^H . For circuits with 5 or less Hadamard gates, depth is minimized by solution \mathcal{S}_{low}^H , for 15 or more it is best to use \mathcal{S}_{high}^H . The remaining one of the four solutions \mathcal{S}_{sub}^H is sub-optimal in all regions, so it can be eliminated from the set of solution candidates. Interestingly, as k increases, the difference between the three remaining solutions becomes more pronounced in the respective Hadamard regions.

Above insights motivate us to use different LCS solutions for different Hadamard counts, which we refer to in the following as the *piecewise-best selection* strategy. Evaluations show that for $k > 10$, the crossover points are the following:

$$\begin{aligned} &\text{Use } \mathcal{S}_{low}^H \text{ for } 0 < h < \frac{k}{4}, \\ &\text{use } \mathcal{S}_{mid}^H \text{ for } \frac{k}{4} \leq h \leq \frac{3k}{4}, \\ &\text{use } \mathcal{S}_{high}^H \text{ for } \frac{3k}{4} < h < k. \end{aligned} \quad (4)$$

Following the case distinction in Eq. (4), the optimal compilation strategy can be selected purely based on the Hadamard count and size of the C-QSK of interest. However, currently, for each circuit we still have to use the LCS algorithm to produce the desired logical realization. This is highly impractical, in particular for larger system sizes. We eliminate this inefficiency by generalizing the solution primitives to explicit closed-form compilation strategies in the next section.

IV. GENERALIZED COMPILE STRATEGY FOR ARBITRARY SYSTEM SIZES

In this section, we generalize the three solution primitives $\mathcal{S}_{low}^H, \mathcal{S}_{mid}^H, \mathcal{S}_{high}^H$ identified in Sec. III to actual compilation strategies $\mathcal{C}_{low}^H, \mathcal{C}_{mid}^H, \mathcal{C}_{high}^H$. Therefore, we systematically examine the logical circuit structures for small system sizes k and different Hadamard counts h to extract repeating patterns. This

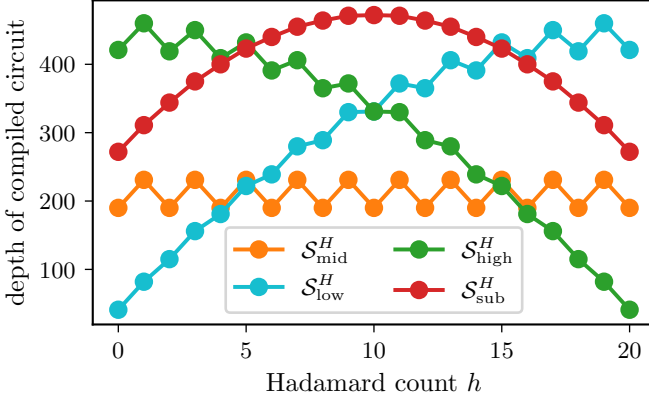


Fig. 3: Comparison of depth for logical realizations of C-QSKs on varying system sizes as a function of the Hadamard count h . We plot the four position-invariant solutions of LCS for C-QSK circuits on $k = 20$ qubits. While solution S_{mid}^H produces particularly shallow circuits in the regime of about 5 to 15 Hadamard gates, S_{low}^H is clearly superior in case of sparse and S_{high}^H for dense Hadamard placement.

enables us to describe four main building blocks, from which every circuit is composed, schematically shown for $k = 4$ in Fig. 4. In the following, we derive closed-form descriptions for the three compilation strategies, depending on Hadamard density. To streamline presentation and make subsequent calculations cleaner and more concise, we first introduce a few shorthand notations: Let G denote an arbitrary single-qubit gate. For an index set $I \subseteq [n]$, we define the corresponding single-qubit gate layer by

$$G_I := \prod_{i \in I} G_i. \quad (5)$$

For two index sets $I_1, I_2 \subseteq [n]$, we define a CZ block acting on all pairs $(i, j) \in I_1 \times I_2$ as

$$\text{CZ}_{(i,j) \in I_1 \times I_2} := \prod_{i \in I_1} \prod_{j \in I_2} \text{CZ}_{i,j}. \quad (6)$$

Analogously, for a CNOT block with controls on I_1 and targets on I_2 , we define

$$\text{CX}_{i \in I_1 \rightarrow j \in I_2} := \prod_{i \in I_1} \prod_{\substack{j \in I_2 \\ j \neq i}} \text{CX}_{i \rightarrow j}. \quad (7)$$

A. Compilation Strategy for Moderate Hadamard Counts

To determine the optimal compilation strategy for moderate Hadamard counts, interpreted as the range defined in Eq. (4), we analyze the four building blocks identified in Fig. 4 for instances of size $k = 4$. However, we note that the same structures generalize to systems of arbitrary size, as we also prove at the end of this section.

In Fig. 5(a) we show representative logical realizations of the first block, with the sets $\mathcal{E}(I_h)$ and $\mathcal{E}(\bar{I}_h)$ highlighted

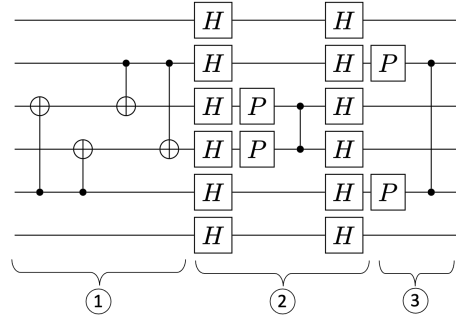
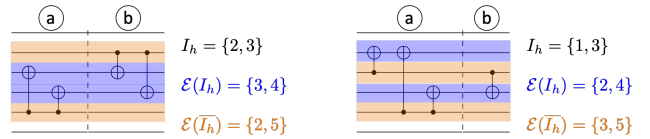
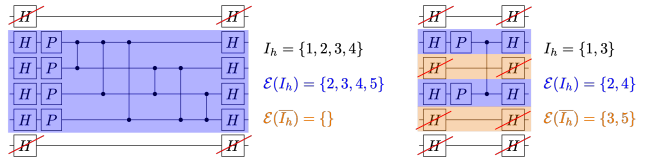


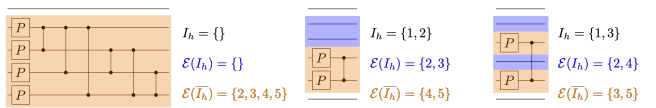
Fig. 4: Building blocks for logical realizations of C-QSKs with even Hadamard count: (1) CNOT-entanglement layer, (2) IQP-like structure, (3) Z-diagonal layer. While shown for $k = 4$, the same structure is observed for all system sizes. The concrete instantiation of the blocks depends on the Hadamard count, position, and the choice of strategy \mathcal{S} .



(a) Two instances of the first block from Fig. 4: the targets of the CNOT operations are wires in $\mathcal{E}(I_h)$, while the controls lie in the disjoint set $\mathcal{E}(\bar{I}_h)$. The structure is subdivided into CNOT operations with (a) control wire indices larger than target wire indices and (b) vice versa. Overall, this observation is summarized in Eq. (8). Note that $I_h, \bar{I}_h \subseteq [k]$.



(b) Two instances of the second block from Fig. 4: the first and last layer contain Hadamard gates on all wires. In between, P gates (CZ gates) act on all (pairs of) wires in the index set $\mathcal{E}(I_h)$. With some of the Hadamard gates canceling to identity, we arrive at Eq. (9).



(c) Three instances of the third block from Fig. 4: P gates (CZ gates) act on all (pairs of) wires in the index set $\mathcal{E}(\bar{I}_h)$, yielding Eq. (10).

Fig. 5: Exemplary instances of the three blocks from Fig. 4, corresponding to LCS solution S_{mid}^H . The underlying C-QSK circuits are of size $k = 4$ and contain an even number of Hadamard gates. Based on just these few instances, it is possible to compactly formulate the compilation strategy in Eqs. (8) to (10). The full compilation strategy C_{mid}^H just sequentially concatenates the three compiled blocks.

in blue and red, respectively. It is evident that the CNOT-targets lie on $\mathcal{E}(I_h)$, while the controls act on $\mathcal{E}(\bar{I}_h)$. Moreover, the CNOT-structure can be divided into two parts: First, all CNOTs are applied with control indices larger

than their targets, while in the second part, the order is reversed, with controls smaller than the targets. This decomposition can be expressed as (a) $\text{CX}_{i \in \mathcal{E}(\overline{I_h}) \rightarrow \substack{j \in \mathcal{E}(I_h) \\ j < i}}$ and (b) $\text{CX}_{i \in \mathcal{E}(\overline{I_h}) \rightarrow \substack{j \in \mathcal{E}(I_h) \\ j > i}}$, which we summarize into

$$\text{CX}_{\mathcal{E}(\overline{I_h}) \rightarrow \mathcal{E}(I_h)}. \quad (8)$$

Similar regularities can be identified in the second block consisting of an IQP-like structure [23], as shown in Fig. 5(b). First, many of the Hadamard cancel since $H^2 = \mathbb{I}$. The remaining Hadamard gates always occupy the wires with indices in $\mathcal{E}(I_h)$. The same applies to the consecutive layer of P gates. Finally, both controls and targets of the CZ gates are restricted to unordered combinations from $\mathcal{E}(I_h)$. Altogether, the structure can be summarized by the following sequence:

$$H_{\mathcal{E}(I_h)} \cdot P_{\mathcal{E}(I_h)} \cdot \text{CZ}_{\{(i,j) \in \mathcal{E}(I_h)^2 \mid j > i\}} \cdot H_{\mathcal{E}(I_h)} \quad (9)$$

We now turn our attention to the third and final structural block of the compiled circuit: a Z-diagonal layer consisting of P gates followed by CZ gates. In contrast to the second block, these gates operate solely on wires with indices in $\mathcal{E}(\overline{I_h})$. This behavior can be summarized by the following product rules:

$$P_{\mathcal{E}(\overline{I_h})} \cdot \text{CZ}_{\{(i,j) \in \mathcal{E}(\overline{I_h})^2 \mid j > i\}}, \quad (10)$$

where the first factor represents the application of P gates across all wires in $\mathcal{E}(\overline{I_h})$, while the second one indicates a layer of CZ gates acting pairwise within $\mathcal{E}(\overline{I_h})$.

Interestingly, by combining all three building blocks, we recover the same gate sequencing rule as obtained by the SAS method, which is depicted in Fig. 2. The case for odd Hadamard gates works analogously to the above, for which the same equivalence observation could be made. However, compared to the approach in the original SAS paper [11], above derivation follows a much more straightforward and intuitive paradigm: instead of going through the intricate procedure of stitching together root circuits derived from Pauli constraints and subsequently applying logical identities to simplify the circuit and reduce its depth, we directly identify simple structural rules for the constituent blocks and compose them.

As the methodology for deriving the two other compilation strategies $\mathcal{C}_{\text{low}}^H$ and $\mathcal{C}_{\text{high}}^H$ is the same as above, we defer them to App. A.

In order to prove that the derived constructions are indeed logical realizations, it remains to be shown that the gate-sequencing rules satisfy two key requirements: they implement the desired logical mapping of the C-QSK and preserve the stabilizers on the $[[n, n-2, 2]]$ code. We state respective theorems in the following and defer the straightforward but laborious proofs to App. B.

Theorem 1. *The compilation strategies $\mathcal{C}_{\text{low}}^H, \mathcal{C}_{\text{mid}}^H, \mathcal{C}_{\text{high}}^H$ satisfy the physical Pauli constraints for any C-QSK circuit.*

Theorem 2. *The compilation strategies $\mathcal{C}_{\text{low}}^H, \mathcal{C}_{\text{mid}}^H, \mathcal{C}_{\text{high}}^H$ preserve the $[[n, n-2, 2]]$ code stabilizers $X_{[n]}$ and $Z_{[n]}$.*

With that, we derived provably correct and stabilizer-preserving compilation strategies $\mathcal{C}_{\text{low}}^H, \mathcal{C}_{\text{mid}}^H, \mathcal{C}_{\text{high}}^H$ which are depth-optimized for varying Hadamard counts. As the $\mathcal{C}_{\text{mid}}^H$ compilation strategy is equivalent to the SAS approach in Fig. 2, for the mid-regime in Eq. (4), both methods produce compiled circuits of the same depth. However, as shown in Sec. III for sparse and dense Hadamard placement, one can significantly improve depth by switching to other strategies $\mathcal{C}_{\text{low}}^H, \mathcal{C}_{\text{high}}^H$. With that, we emphasize that the combination of the three strategies allows for the realization of the *piecewise-best selection* (PBS) compiler introduced in Sec. III, which we will empirically evaluate in the following.

V. EMPIRICAL EVALUATION

In this section, we empirically evaluate the PBS compilation strategy with the selection terms given in Eq. (4) switching between $\mathcal{C}_{\text{low}}^H, \mathcal{C}_{\text{mid}}^H$, and $\mathcal{C}_{\text{high}}^H$, respectively. For the experiments, we implemented compilation, noise simulation, and evaluation of C-QSKs on the $[[n, n-2, 2]]$ code using Qiskit [24]. The simulations are conducted using the AerSimulator with the extended-stabilizer method.

The evaluation procedure is given a system size k , a Hadamard-position set I_h , and depolarizing noise rates p_1 and p_2 (non-correlated for single-qubit gates and correlated for two-qubit gates, respectively). We then generate a logical C-QSK circuit both via the SAS approach and using our PBS compilation strategy. The assembled pipeline comprises QEC encoder, the respective *logical C-QSK* realization, *syndrome detection*, and *measurement* of both data wires and stabilizers. To isolate the effect of noise on the logical computation, the encoder is compiled into a single Clifford instruction and treated as noiseless, and the syndrome extraction and measurement stage is likewise assumed ideal.

The syndrome-detection measurement, together with the data readout yields empirical distributions over outcomes of the form (x, s) , where $x \in \{0, 1\}^n$ is the n -bit string obtained from the data register, and $s \in \{00, 01, 10, 11\}$ is the two-bit syndrome string obtained from the stabilizer measurement. We define the *acceptance rate* p_{acc} as the fraction of outcomes, for which the syndrome yields 00. Complimentarily, the *success rate* p_{succ} is the fraction of runs, where the 00 syndrome is observed, and there was actually no fault in the computation.

For a system size of $k = 20$ and noise strength $p_1 = 0.01$ and $p_2 = 0.01$ we compare p_{acc} and p_{succ} resulting from SAS and PBS compilation in Fig. 6. As suggested by the equivalence of SAS and the compilation strategy $\mathcal{C}_{\text{mid}}^H$ selected by PBS for moderate Hadamard counts (see Eq. (4)), for $6 \leq h \leq 14$ both methods are on par up to minor statistical fluctuations. However, in the edge regimes, i.e. low Hadamard counts $h \leq 5$ and high counts $h \geq 15$, the strategies $\mathcal{C}_{\text{low}}^H$ and $\mathcal{C}_{\text{high}}^H$ are selected by PBS, respectively. For these circuit structures, one can observe a significantly higher p_{acc} and p_{succ} , likely caused by the shallower logical realization and two-qubit count being the dominant error driver in realistic mid-term setups. Empirically, we observed that for larger k the differences between SAS and PBS in the edge regimes become even more

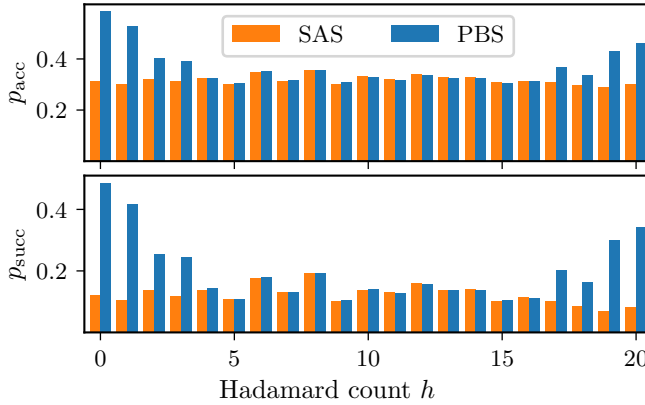


Fig. 6: Comparison of SAS and PBS compilation strategies for C-QSKs on $k = 20$ qubits across Hadamard counts h . We analyze the (upper plot) acceptance rate p_{acc} and the (lower plot) success rate p_{succ} , identifying advantages of PBS in the edge regimes of sparse and dense Hadamard placements.

pronounced, highlighting the promise of the newly introduced compilation strategy.

VI. DISCUSSION AND OUTLOOK

In this work, we introduced a novel technique for the logical compilation of Clifford circuits on particular code families. Starting with small Clifford quantum simulation kernel (C-QSK) instances, we enumerated the full *logical Clifford synthesis* (LCS) solution space [10], profiled depth and two-qubit counts across circuit configurations, and extracted depth-favorable compilation primitives. We then distilled these components into compilation strategies that generalize to arbitrary system sizes, yielding the *piecewise-best selection* (PBS) routine that lowers two-qubit gate counts relative to *solve-and-stitch* (SAS) [11], [12], which itself already significantly improved upon gate-by-gate compilation. The gains are particularly prevalent for C-QSK with sparse and dense Hadamard placements. In our noise studies, we identified circuit depth as the dominant driver of logical performance; correspondingly, due to reduced two-qubit gate count, we also observed significant improvements in success probability.

Despite these promising insights, limitations remain: the method is demonstrated on the $[[n, n-2, 2]]$ code family (supporting error detection but not correction), focuses on C-QSK and thus Clifford circuits, and does not yet enforce full fault tolerance. We view the first two as matters of scope rather than principle: because our workflow mines small instances and generalizes primitives into closed-form templates verified by Pauli-constraint and stabilizer-preservation checks, it can be applied to other code families with higher distances. The same flexibility allows broadening beyond C-QSK to other Clifford subroutines, enhancing usefulness in a peephole optimization workflow. While the approach does not generalize to arbitrary non-Clifford routines, it may extend to circuits with limited non-Clifford components, e.g., a single T gate within the quantum simulation kernel. However, such considerations

are beyond the scope of this work. The third limitation, i.e. lack of enforced fault tolerance can be addressed by embedding flag gadgets [17], as demonstrated in [11].

In summary, our approach provides a compact and extensible tool for improving peephole-based logical compilation: it identifies compilation primitives on small instances and generalizes these with limited hand-crafting overhead to scalable compilation strategies.

ACKNOWLEDGMENT

We thank N. Rengaswamy and Z. Chen for insightful discussions of their work, which inspired this study. We furthermore thank J. Jordan for administrative support and constructive feedback.

CODE AVAILABILITY

The code supporting this study is currently undergoing final polishing and will be released publicly at a later stage. Further information and data is available upon reasonable request.

APPENDIX

A. Other Compilation Strategies for Piecewise-Best Selection

In the following, we derive the compilation strategies $\mathcal{C}_{\text{low}}^H$ for low Hadamard count in App. A1 and $\mathcal{C}_{\text{high}}^H$ for high Hadamard count in App. A2. In large parts, the methodology is the same as in Sec. IV-A, but a few additional insights are introduced. As already explained in the main part, the combination of the three compilation strategies allows us to define the *piecewise-best selection* (PBS) strategy, which produces depth-optimized logical realizations in all Hadamard regimes.

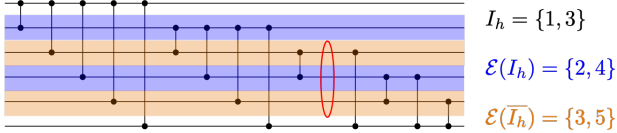
1) *Compilation Strategy for Low Hadamard Counts:* While the derivations only slightly differ, there are different structural patterns for Clifford quantum simulation kernels (C-QSKs) with even and with odd Hadamard count, which we consider separately in the following:

Even number of Hadamard gates. Comparing circuits generated with $\mathcal{S}_{\text{low}}^H$ to $\mathcal{S}_{\text{mid}}^H$, we observe that the first two blocks (i.e. the CNOT-entanglement layer and the IQP-like structure) are identical and thus follow Eqs. (8) and (9). The only difference lies in the final Z-diagonal block, where the additional P -layer follows the rule

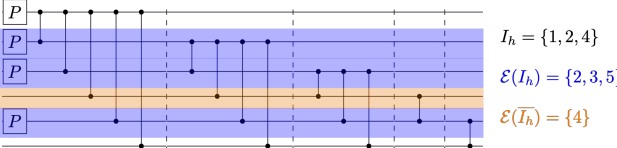
$$P_{[n] \setminus \mathcal{E}(\overline{I_h})}, \quad (11)$$

that is, P gates are applied on all wires except those belonging to $\mathcal{E}(\overline{I_h})$. For the CZ-structure, instead of directly analyzing which sequencing rules generate the circuit blocks, it is more instructive to examine what is missing compared to the fully connected block. For the instance shown in Fig. 7(a), exactly those CZ gates whose control and target both lie in $\mathcal{E}(\overline{I_h})$ are absent. The missing gate is highlighted by the red oval. This pattern holds systematically for all C-QSKs, leading to the following compact formula:

$$\text{CZ}_{\{(i,j) \in [n]^2 \setminus \mathcal{E}(\overline{I_h})^2 \mid j > i\}} \quad (12)$$



(a) Part of third block of Fig. 4 for even Hadamard count. Compared to the fully connected instance, the CZ gate on the wire pair $E(\overline{I_h})^2 = \{(3, 5)\}$ is omitted, yielding Eq. (12).



(b) Third block of Fig. 4 for odd Hadamard count. The P -layer acts on the first wire and wires in $E(I_h)$. Wire by wire, if the upper control lies in $[n] \setminus E(I_h)$, all lower qubits are targeted by CZ gates; otherwise, an upper qubit in $E(I_h)$ couples via CZ only to qubits in $E(I_h)$, yielding Eq. (16).

Fig. 7: Exemplary instances of the blocks from Fig. 4, corresponding to *logical Clifford synthesis* (LCS) solution $\mathcal{S}_{\text{low}}^H$. The underlying C-QSK circuits are of size $k = 4$.

Combining Eqs. (11) and (12) gives us the sequencing rule for the third block of $\mathcal{C}_{\text{low}}^H$ in the case of even Hadamard count.

Odd number of Hadamard gates. As before, the first and second block in this case are identical to the strategy for $\mathcal{S}_{\text{mid}}^H$. Analyzing representative examples in Fig. 7(b), we get the sequencing formula for the P gates as

$$P_{i \in \{1\} \cup E(I_h)}. \quad (13)$$

Adopting the convention that for each CZ gate the control is the upper wire and the target on the lower wire, the following pattern holds: for every wire $i \in [n] \setminus E(\overline{I_h})$ we obtain

$$CZ_{\{(i,j) \in \{i\} \times [n] \mid j > i\}}, \quad (14)$$

while for every wire $i \in E(\overline{I_h})$ we obtain the block

$$CZ_{\{(i,j) \in \{i\} \times E(I_h) \mid j > i\}}. \quad (15)$$

In Fig. 7(b), these two types of blocks are separated by dashed lines. By iterating through all wires, the complete sequencing rule for this block can be written as

$$CZ_{\{(i,j) \in [n] \setminus E(\overline{I_h}) \times [n] \mid j > i\}} \cdot CZ_{\{(i,j) \in E(\overline{I_h}) \times E(I_h) \mid j > i\}}, \quad (16)$$

which combined with Eq. (13) completes the set of sequencing rules for $\mathcal{C}_{\text{low}}^H$.

2) Compilation Strategy for High Hadamard Counts: As the derivations for $\mathcal{C}_{\text{high}}^H$ follow the same ideas as for $\mathcal{C}_{\text{low}}^H$ and $\mathcal{C}_{\text{mid}}^H$, we directly state the sequencing rules in the following.

Even number of Hadamard gates. The sequencing rules for the first and third block are identical between $\mathcal{C}_{\text{mid}}^H$ and $\mathcal{C}_{\text{high}}^H$. For the second layer, it is easy to see that Hadamard gates are applied on every wire $i \in [n]$ and that the P gates act only on wires in $[n] \setminus E(I_h)$, which yields

$$H_{[n]} \quad \text{and} \quad P_{[n] \setminus E(I_h)}. \quad (17)$$

Proceeding as above and comparing the CZ structure with the fully connected circuit, we obtain

$$CZ_{\{(i,j) \in [n]^2 \setminus E(I_h)^2 \mid j > i\}}. \quad (18)$$

Odd number of Hadamard gates. This last case just replaces the sequencing rules for the second layer with

$$H_{[n]} \quad \text{and} \quad P_{E(\overline{I_h}) \cup \{n\}}, \quad (19)$$

as well as

$$CZ_{\{(i,j) \in [n]^2 \setminus ((E(I_h) \cup \{1\}) \times E(I_h))\}}. \quad (20)$$

B. Proof of Theorems

In the following, we prove Theorems 1 and 2 showing the correctness of the compilation strategies we derived.

1) Physical Pauli Constraints:

Theorem. *The compilation strategies $\mathcal{C}_{\text{low}}^H, \mathcal{C}_{\text{mid}}^H, \mathcal{C}_{\text{high}}^H$ satisfy the physical Pauli constraints for any C-QSK circuit.*

We explicitly execute the proof for $\mathcal{C}_{\text{mid}}^H$ in the case of an even number of Hadamard gates and for cases where $k \in E(\overline{I_h})$ is the mapping relation for the physical operators $X_1 X_k$, which is given by

$$X_1 X_k \mapsto \begin{cases} X_1 X_k, & k \in E(I_h), \\ X_1 Y_k X_{E(I_h)} Z_{E(\overline{I_h}) \setminus \{k\}}, & k \in E(\overline{I_h}). \end{cases} \quad (21)$$

All remaining mapping relations, namely the case $k \in E(I_h)$ for $X_1 X_k$, the relations for $Z_k Z_n$ for both $k \in E(I_h)$ and $k \in E(\overline{I_h})$, the corresponding cases for an odd number of Hadamard gates, as well as the other compilation strategies $\mathcal{C}_{\text{low}}^H, \mathcal{C}_{\text{high}}^H$, can be shown in complete analogy by following the same procedure.

Proof. The first gate block of the operator $X_1 X_k$ is conjugated by $\text{CX}_{E(I_h) \rightarrow E(\overline{I_h})}$:

$$\text{CX}_{E(I_h) \rightarrow E(\overline{I_h})} (X_1 X_k) \text{CX}_{E(I_h) \rightarrow E(\overline{I_h})} = X_1 X_k X_{E(\overline{I_h})} \quad (22)$$

The conjugation with the $H_{E(I_h)}$ and $P_{E(I_h)}$ layer only effects qubits on the $E(I_h)$ wires, hence

$$P_{E(I_h)} H_{E(I_h)} (X_1 X_k X_{E(I_h)}) H_{E(I_h)} P_{E(I_h)} = X_1 X_k Z_{E(I_h)}. \quad (23)$$

The conjugation by $\text{CZ}_{\{(i,j) \in E(I_h)^2 \mid j > i\}}$ has no effect on $X_1 X_k Z_{E(I_h)}$, since qubits 1 and k lie outside $E(I_h)$ and Z gates commute with CZ gates. The subsequent $H_{E(I_h)}$ transforms $Z_{E(I_h)}$ into $X_{E(I_h)}$, acting only on qubits in $E(I_h)$. Next, $P_{E(\overline{I_h})}$ acts only on X_k (because $1 \notin E(\overline{I_h})$ and $E(I_h) \cap E(\overline{I_h}) = \emptyset$) and turns it into Y_k . Hence, before the final CZ -block, the operator becomes $X_1 Y_k X_{E(I_h)}$. Conjugation by $\text{CZ}_{\{(i,j) \in E(\overline{I_h})^2 \mid j > i\}}$ then yields

$$\begin{aligned} & \text{CZ}_{\{(i,j) \in E(\overline{I_h})^2 \mid j > i\}} (X_1 Y_k X_{E(I_h)}) \text{CZ}_{\{(i,j) \in E(\overline{I_h})^2 \mid j > i\}} \\ &= X_1 Y_k Z_{E(\overline{I_h}) \setminus \{k\}} X_{E(I_h)}. \end{aligned} \quad (24)$$

□

2) Stabilizer Preservation:

Theorem. The compilation strategies $\mathcal{C}_{low}^H, \mathcal{C}_{mid}^H, \mathcal{C}_{high}^H$ preserve the $[[n, n-2, 2]]$ code stabilizers $X_{[n]}$ and $Z_{[n]}$.

We show the proof for X -type stabilizer on \mathcal{C}_{mid}^H , while the proofs for the Z -type stabilizer and respective versions for $\mathcal{C}_{low}^H, \mathcal{C}_{high}^H$ can be done in complete analogy.

Proof. To prove the preservation of the stabilizer $X_{[n]} = X_1 X_{\mathcal{E}(I_h)} X_{\mathcal{E}(\overline{I_h})} X_n$, we have to perform the same procedure on this operator as before. Conjugating $X_{[n]}$ by $\text{CX}_{\mathcal{E}(\overline{I_h}) \rightarrow \mathcal{E}(I_h)}$ we only have to analyze its working on $X_{\mathcal{E}(I_h)} X_{\mathcal{E}(\overline{I_h})}$ since $1, n \notin \mathcal{E}(I_h), \mathcal{E}(\overline{I_h})$. Here, we have

$$\begin{aligned} & \text{CX}_{\mathcal{E}(\overline{I_h}) \rightarrow \mathcal{E}(I_h)} X_{\mathcal{E}(I_h)} X_{\mathcal{E}(\overline{I_h})} \text{CX}_{\mathcal{E}(\overline{I_h}) \rightarrow \mathcal{E}(I_h)} \\ &= (\text{CX}_{\mathcal{E}(\overline{I_h}) \rightarrow \mathcal{E}(I_h)} X_{\mathcal{E}(I_h)} \text{CX}_{\mathcal{E}(\overline{I_h}) \rightarrow \mathcal{E}(I_h)}) \\ & \quad \cdot (\text{CX}_{\mathcal{E}(\overline{I_h}) \rightarrow \mathcal{E}(I_h)} X_{\mathcal{E}(\overline{I_h})} \text{CX}_{\mathcal{E}(\overline{I_h}) \rightarrow \mathcal{E}(I_h)}). \end{aligned} \quad (25)$$

It is $\text{CX}_{\mathcal{E}(\overline{I_h}) \rightarrow \mathcal{E}(I_h)} X_{\mathcal{E}(I_h)} \text{CX}_{\mathcal{E}(\overline{I_h}) \rightarrow \mathcal{E}(I_h)} = X_{\mathcal{E}(I_h)}$ because $\text{CX}_{i \rightarrow j} X_j \text{CX}_{i \rightarrow j} = X_j$ for all $i \in \mathcal{E}(\overline{I_h})$ and $j \in \mathcal{E}(I_h)$. Further, it holds that

$$\begin{aligned} & \text{CX}_{\mathcal{E}(\overline{I_h}) \rightarrow \mathcal{E}(I_h)} X_{\mathcal{E}(\overline{I_h})} \text{CX}_{\mathcal{E}(\overline{I_h}) \rightarrow \mathcal{E}(I_h)} \\ &= \prod_{i \in \mathcal{E}(\overline{I_h})} X_i X_{\mathcal{E}(I_h)} = X_{\mathcal{E}(\overline{I_h})} \underbrace{X_{\mathcal{E}(I_h)}^{|\mathcal{E}(\overline{I_h})|}}_{= \mathbb{I}} = X_{\mathcal{E}(\overline{I_h})} \end{aligned} \quad (26)$$

showing that the CNOT block leaves the X stabilizer invariant. Application of $H_{\mathcal{E}(I_h)}$ and then $P_{\mathcal{E}(I_h)}$ effects only the $X_{\mathcal{E}(I_h)}$ gates in the stabilizers turning it into $Z_{\mathcal{E}(I_h)}$. Further application of the $\text{CZ}_{\{(i,j) \in \mathcal{E}(I_h)^2 | j > i\}}$ block on the conjugated X -stabilizers has no effect since $1, n \notin \mathcal{E}(I_h)$ and $\mathcal{E}(I_h), \mathcal{E}(\overline{I_h})$ are disjoint sets. Conjugation again with $H_{\mathcal{E}(I_h)}$ transforms $Z_{\mathcal{E}(I_h)}$ back to $X_{\mathcal{E}(I_h)}$ and $P_{\mathcal{E}(\overline{I_h})}$ turns $X_{\mathcal{E}(\overline{I_h})}$ into $Y_{\mathcal{E}(\overline{I_h})}$, hence in total we have $X_1 X_{\mathcal{E}(I_h)} Y_{\mathcal{E}(\overline{I_h})} X_n$. The last conjugation with the $\text{CZ}_{\{(i,j) \in \mathcal{E}(\overline{I_h})^2 | j > i\}}$ block acts only on $Y_{\mathcal{E}(\overline{I_h})}$. First, we rewrite the CZ-block in the following way:

$$\text{CZ}_{\{(i,j) \in \mathcal{E}(\overline{I_h})^2 | j > i\}} = \prod_{\substack{M \in \mathcal{M}(\mathcal{E}(\overline{I_h})) \\ (i,j) \in M}} \text{CZ}_{i,j} \quad (27)$$

Here, $\mathcal{M}(\mathcal{E}(\overline{I_h}))$ is the set of all perfect matchings for the graph $G(V, E)$ with $V = \mathcal{E}(\overline{I_h})$ and $E = \{(i, j) | i < j\}$. The graph is complete, hence the number of perfect matchings is odd. For an $M \in \mathcal{M}(\mathcal{E}(\overline{I_h}))$, it is

$$\text{CZ}_M Y_{\mathcal{E}(\overline{I_h})} \text{CZ}_M = (-1)^{|M|} X_{\mathcal{E}(\overline{I_h})}, \quad (28)$$

$$\text{CZ}_M X_{\mathcal{E}(\overline{I_h})} \text{CZ}_M = (-1)^{|M|} Y_{\mathcal{E}(\overline{I_h})}. \quad (29)$$

Furthermore, we use the fact that for two indices $i, j \in \mathcal{E}(\overline{I_h})$, it holds that $\text{CZ}_{i,j} Y_i Y_j \text{CZ}_{i,j} = -X_i X_j$ and $\text{CZ}_{i,j} X_i X_j \text{CZ}_{i,j} = -Y_i Y_j$. So applying the CZ-block from Eq. (27) on $Y_{\mathcal{E}(\overline{I_h})}$ corresponds to a repeated application of CZ_M blocks with $M \in \mathcal{M}(\mathcal{E}(\overline{I_h}))$ an odd number of times, which results in $(\pm 1) X_{\mathcal{E}(I_h)}$, hence one can conclude the preservation of the X-stabilizer. \square

REFERENCES

- [1] P. W. Shor, “Scheme for reducing decoherence in quantum computer memory,” *Phys. Rev. A*, vol. 52, no. 4, p. R2493, 1995.
- [2] Google Quantum AI, “Quantum error correction below the surface code threshold,” *Nature*, vol. 638, no. 8052, p. 920, 2025.
- [3] D. Gottesman, “An Introduction to Quantum Error Correction and Fault-Tolerant Quantum Computation,” *arXiv:0904.2557*, 2009.
- [4] D. Litinski, “A Game of Surface Codes: Large-Scale Quantum Computing with Lattice Surgery,” *Quantum*, vol. 3, p. 128, 2019.
- [5] D. Horsman, A. G. Fowler, S. Devitt, and R. V. Meter, “Surface code quantum computing by lattice surgery,” *New J. Phys.*, vol. 14, no. 12, p. 123011, 2012.
- [6] C. Gidney and A. G. Fowler, “Efficient magic state factories with a catalyzed $|CCZ\rangle$ to $|2T\rangle$ transformation,” *Quantum*, vol. 3, p. 135, 2019.
- [7] D. Gottesman, “Theory of fault-tolerant quantum computation,” *Phys. Rev. A*, vol. 57, no. 1, p. 127137, 1998.
- [8] A. R. Calderbank and P. W. Shor, “Good quantum error-correcting codes exist,” *Physical Review A*, vol. 54, no. 2, p. 10981105, 1996.
- [9] J. Dehaene and B. De Moor, “Clifford group, stabilizer states, and linear and quadratic operations over $GF(2)$,” *Phys. Rev. A*, vol. 68, no. 4, p. 042318, 2003.
- [10] N. Rengaswamy, R. Calderbank, H. D. Pfister, and S. Kadhe, “Synthesis of Logical Clifford Operators via Symplectic Geometry,” in *IEEE International Symposium on Information Theory (ISIT)*, 2018, p. 791.
- [11] Z. Chen and N. Rengaswamy, “Tailoring Fault-Tolerance to Trotter Circuits,” in *IEEE International Conference on Quantum Computing and Engineering (QCE)*, vol. 1, 2024, p. 134.
- [12] Z. Chen and N. Rengaswamy, “Tailoring Fault-Tolerance to Quantum Algorithms,” *IEEE J. Sel. Areas Inf. Theory*, vol. 6, p. 311, 2025.
- [13] G. Li, A. Wu, Y. Shi, A. Javadi-Abhari, Y. Ding, and Y. Xie, “Pauli-hedral: a generalized block-wise compiler optimization framework for Quantum simulation kernels,” in *ACM International Conference on Architectural Support for Programming Languages and Operating Systems (ASPLOS)*, 2022, p. 554.
- [14] Z. Chen, J. O. Weinberg, and N. Rengaswamy, “Fault Tolerant Quantum Simulation via Symplectic Transvections,” in *IEEE International Conference on Quantum Computing and Engineering (QCE)*, 2025, p. 158.
- [15] J. Liu, L. Bello, and H. Zhou, “Relaxed Peephole Optimization: A Novel Compiler Optimization for Quantum Circuits,” in *IEEE/ACM International Symposium on Code Generation and Optimization (CGO)*, vol. 01, 2021, p. 301.
- [16] S. Rietsch, A. Y. Dubey, C. Utrecht, M. Periyasamy, A. Plinge, C. Mutschler, and D. D. Scherer, “Unitary Synthesis of Clifford+T Circuits with Reinforcement Learning,” in *IEEE International Conference on Quantum Computing and Engineering (QCE)*, vol. 1, 2024, p. 824.
- [17] R. Chao and B. W. Reichardt, “Fault-tolerant quantum computation with few qubits,” *npj Quantum Inf.*, vol. 4, no. 1, p. 42, 2018.
- [18] L. Paletta, A. Leverrier, A. Sarlette, M. Mirrahimi, and C. Vuillot, “Robust sparse IQP sampling in constant depth,” *Quantum*, vol. 8, p. 1337, 2024.
- [19] D. Hangleiter, M. Kalinowski, D. Bluvstein, M. Cain, N. Maskara, X. Gao, A. Kubica, M. D. Lukin, and M. J. Gullans, “Fault-Tolerant Compiling of Classically Hard Instantaneous Quantum Polynomial Circuits on Hypercubes,” *PRX Quantum*, vol. 6, no. 2, p. 020338, 2025.
- [20] N. Meyer, C. Mutschler, A. Maier, and D. D. Scherer, “Learning Encodings by Maximizing State Distinguishability: Variational Quantum Error Correction,” *arXiv:2506.11552*, 2025.
- [21] N. Meyer, C. Mutschler, A. Maier, and D. D. Scherer, “Variational Quantum Error Correction,” in *IEEE International Conference on Quantum Computing and Engineering (QCE)*, vol. 2, 2025, p. 456.
- [22] J. Bausch, A. W. Senior, F. J. Heras, T. Edlich, A. Davies, M. Newman, C. Jones, K. Satzinger, M. Y. Niu, S. Blackwell *et al.*, “Learning high-accuracy error decoding for quantum processors,” *Nature*, vol. 635, no. 8040, p. 834, 2024.
- [23] D. Shepherd and M. J. Bremner, “Temporally unstructured quantum computation,” *Proceedings of the Royal Society*, vol. 465, no. 2105, p. 1413, 2009.
- [24] Qiskit contributors, “Qiskit: An open-source framework for quantum computing,” 2026.